

Full Length Research Paper

The mRNA quantitative analysis, prokaryotic expression and structure prediction of hepatocarcinogenesis related gene *idh3* under AFB₁ stress

Zhuang Zhenhong, Zhang Feng, Li Yanyun, Yuan Jun, Yang Yanling, Lin Ling and Wang Shihua*

Key Laboratory of Biopesticide and Chemical Biology, Ministry of Education, and College of Life Sciences, Fujian Agriculture and Forestry University, Fuzhou 350002, China.

Accepted 19 February, 2019

By differential proteomics analysis, it was found that the expression level of IDH3 (Isocitrate dehydrogenase 3) in mouse liver was significantly increased under the stress of Aflatoxin B₁. To validate the result of differential proteomics analysis, fluorescence quantitative PCR was used to detect the changing trend of *idh3* mRNA volume induced by Aflatoxin B₁ in mouse liver. The result showed that the expression volume of *idh3* mRNA showed an increasing trend with the increase of Aflatoxin B₁ concentration, which corresponded with the result of differential proteomics analysis. The prokaryotic expression vector for *idh3* was constructed in the study with pET28a as a recipient plasmid. The expression vector (pET28a-*idh3*) was used to transform BL21, after which the positive expression strain (*Escherichia coli* BL21/pET28a-*idh3*) was induced to express with 100 mmol/L IPTG under 28°C for 4 h, and the prokaryotic expression product of IDH3 was successfully detected by SDS-PAGE electrophoresis. The molecule structure of IDH3 was predicted by bioinformatics analysis, and the results showed that the total number of negatively and positively charged residues were 42 and 39, respectively. Five hydrophobic domains were predicted in the protein, and its average hydrophobicity was -0.069. There was 43% α -helix and 20% β -pleated sheet in the molecule, and the tertiary structure of IDH3 was constituted by 12 α -helices and 12 β -pleated sheets. Based on the results of bioinformatics analysis, the fragments of 1-17 and 112-123 residues of IDH3 were selected as candidates for further effective polyclonal antibody preparation. The results of this study paved way for further exploration of the role of *idh3* in the process of liver canceration induced by Aflatoxin B₁.

Key words: IDH3, aflatoxin B₁, liver, canceration, bioinformatics analysis.

INTRODUCTION

Aflatoxins are one of the secondary metabolites produced by toxigenic fungi, such as *Aspergillus flavus* and *Aspergillus parasiticus*, through polyketide pathway. It is more toxic and carcinogenic and more harmful to human and animals than that of any other natural contaminant

which have been found. Aflatoxin B₁ (AFB₁), which is one kind of aflatoxin, belongs to the liver toxin. Evidence showed that the dose of AFB₁ in food positively correlated with the number of hepatocellular carcinoma case. The possibility of AFB₁ inducing liver canceration (10 g per day) is 75 times as much as that of dimethylnitrosamine (750 g per day) (Leema et al., 2010; Chanda et al., 2009; Yin et al., 2008; Wild et al., 2010; Wogan et al., 1966). For the fact that it was thought to be the main cause of liver cancer, and because low

*Corresponding author. E-mail: wshyy1@sina.com. Tel: +86 (591) 87984471, Fax: +86 (591) 87984471.

concentration of AFB₁ was intaken for a long time with food, the International Agency for Research on Cancer (IARC) of the World Health Organization (WHO) classified AFB₁ as a class 1 carcinogen (Shephard et al., 2003; Williams et al., 2004; IARC, 2002).

IDH3 (NAD-specific isocitrate dehydrogenase, NAD-IDH) is a mitochondria protein by which isocitrate was catalyzed and oxidized to α -ketoglutarate in the citric acid cycle, and is found as a heterotetramer with 2 subunits, 1 subunit, and 1 subunit (Hartong et al., 2008; Hartong et al., 2008; Ramachandran, 1980). IDH3 was found to be downregulated in hCG (human chorionic gonadotropin) induced ovulation in bovine granulosa cells of dominant follicles by the method of SSH (suppression subtractive hybridization), which implied that IDH3 might play a role in the process of follicular growth, ovulation and luteinization (Ndiaye et al., 2005). It was found that cells from *Retinitis pigmentosa* which affected individuals had a significant decrease in IDH3 activity, whereas the activity of NADP-IDH (IDH2) was found to be normal; thus, the findings suggested that the retina has a particular requirement for IDH3 (Hartong et al., 2008).

By the method of differential proteomics analysis and real-time PCR, the over-expression of IDH3 was found to reduce the differentiation of PC12 cells, which implied that IDH3 played a role in neuronal differentiation (Cho et al., 2010). It was concluded from our previous differential proteomics analysis that in the effect of AFB₁ to mice liver, IDH3 was obviously up-regulated with the increase of the intaking amount of AFB₁. According to the result, it was conjectured that IDH3 may play a critical role in the process of liver pathological change or even cancerating under the press of AFB₁. To further test the foregoing result, the changing trend of *idh3* mRNA volume in mouse liver under the press of AFB₁ was detected by fluorescence quantitative PCR. In the study, prokaryon expression system for *idh3* was established, too. The study paved the way to elucidate the function of *idh3* in the cancerating process of liver under AFB₁ stimulation.

MATERIALS AND METHODS

Reagents and apparatus

The reagents used in this study are: fluorescence quantitative PCR kit (purchased from TaKaRa); Reverse transcription kit (purchased from Promega); Trizol extraction kit (purchased from Intrigen); Restriction enzymes, T4 DNA ligase, reagents for PCR (10xTaq Buffer, dNTP, Taq DNA polymerase, and so on) and real-time quantitative PCR kit (purchased from TaKaRa); CIP alkaline phosphatase (purchased from NEB); DNA gel extraction kit (purchased from OMEGA); Single-strand cDNA synthesis kit (purchased from Promega); and Kanamycin, ampicillin and isopropyl- β -D-thiogalactopyranoside (IPTG) (purchased from Amesco). The other chemical reagents used were of analytical grade. Primers were synthesized by Shanghai Sangon Co., Ltd, while the sequence was analyzed by Shanghai Yingjun Biotechnology Co., Ltd.

Experimental materials

A total of 17 male Kunming mice (20 to 25 g per mouse) were purchased from Fujian Medical University. BL21 (DE3) and pET28a(+) were preserved by our lab. The concentration of AFB₁ was 10 μ g/mL in 5% propanediol solution.

Treatment of mice

After a week's feeding, 14 Kunming mice were divided into 5 groups. The negative control group included two mice which were injected intraperitoneally with 300 μ l of 5% propanediol every other day for 4 weeks; while the first, second, third and fourth test group included three mice each, which were injected intraperitoneally with 300 μ l AFB₁ of 5% propanediol solution every other day for 4 weeks, 3 weeks, 2 weeks and 1 week, respectively.

RNA extraction

The liver separated from mice was taken into RNA-enzyme-free glass homogenizer, and was transferred to RNA-enzyme-free 1.5 mL Eppendorf tube after grinding on ice with 1 mL Trizol. The tube was shaken after 200 μ l chloroform per 1 mL Trizol was added, then it was centrifuged at a speed of 12000 r/min for 15 min at 4°C, before the supernatant was transferred to a new non-RNA-enzyme 1.5 mL Eppendorf tube. Isopropyl alcohol was added into the tube at a ratio of 500 μ l per 1 mL Trizol and the solution was mixed by shaking the tube upside down. After stirring for 10 min, it was centrifuged at the conditions of 12000 r/min for 15 min at 4°C, and the supernatant was discarded. The sediment was washed by 80% icy ethanol, and then centrifuged at 12000 r/min for 5 min under 4°C, after which the supernatant was removed. After the Eppendorf tube was put upside down and blown by sterile wind for 15 min, 50 μ l DEPC treated water was added to dissolve the extracted RNA, 5 μ l of which was used to detect RNA purity, while the other amount of treated water was kept under -80°C for the synthesis of the first strand of cDNA.

The synthesis of the first strand of cDNA

Single-stranded cDNA was synthesized according to two-step protocol in the reverse transcription kit from Promega, and was kept under -20°C.

Gene amplification for *idh3*

The primers with conserved sequence were designed according to the cDNA sequence of *idh3* from GeneBank (sense: 5' TATTGAATTCTACGCGATGGCGGGT 3', antisense: 5' TGCCAGGGTCGACAAGTCTTTGACTCTA 3'). There are restriction enzyme sites, *EcoRI* and *SalI*, in the up and down-stream, respectively. The volumes for samples added in PCR reaction were same as those provided in the foregoing. The PCR programme was: 94°C for 5 min, 94°C for 45 s, 57°C for 45 s, 72°C for 1 min, 30 cycles, and extension at 72°C for 5 min. The PCR results were detected by agarose gel electrophoresis, and the corresponding gene fragment was purified by gel extraction purification.

Construction of prokaryotic expression vector pET28a-*idh3*

The plasmids, pET28a and *idh3*, were double digested by *EcoRI* and *SalI*, respectively, after which they were purified by gel extraction purification. After the double-digested pET28a and *idh3* were linked, the

Table 1. Primers used in the study of fluorescence quantitative PCR.

Primer name	Primer sequence	T (°C)	Length of product	Amplified gene
<i>gapdh</i>				
F	5 -ACCCGACCTACCCCTACT-3	64	378 bp	<i>gapdh</i>
R	5 - CATCCCTCCCACAAAGC-3			
<i>idh3</i>				
F	5 -GCCCATTCACGACGACCAA-3	64	256 bp	<i>idh3</i>
R	5 -TAGCACCGCCACTGCCATCC-3			

the recombinant plasmid was transformed into BL21. The positive colonies (*E. coli* BL21/pET28a-*idh3*) were tested by double digestion via restriction enzyme (*EcoRI* and *SaI*), and was sequenced by Shanghai Yingjun Biotechnology Co., Ltd.

Prokaryotic expression for *idh3*

The single colony of the strain, *E. coli* BL21/pET28a-*idh3*, and the negative control strain *E. coli* BL21/pET28a, were cultured respectively. After the OD₆₀₀ of the culture was between 0.4 and 0.6, the IPTG was added to a final concentration of 100 mmol/L. Then, the culture was induced to be expressed under 28°C for 4 h, before it was detected by SDS-PAGE electrophoresis.

Fluorescence quantitative PCR

The primers were designed with the assistance of the software, Primer 5.0, and are shown in Table 1. Reagents preparation for quantitative PCR (total volume: 20 L) is shown as follows: ddH₂O (8.5 L), 2xEXTaq mix (10.0 L), 0.5 L up and down-stream primers, respectively; and 0.5 L template and standard templates which were 5, 25, 125, 625 and 3125-fold diluted respectively by sterile water. Moreover, the PCR program was: Line 1 - 95°C for 30 s; Line 2 - 95°C for 8 s; Line 3 - 64°C for 30 s; Line 4 - Plates read: GOTO Line 2 for 39 times, while the melting curve from 65 to 95°C was read at every 0.2°C for 2 s. When the method of Real Time RT-PCR is used to calculate gene expression volume, it is necessary to choose a housekeeping gene (*gapdh* was chosen in this study) as reference to normalize the test gene - *idh3* (the correction of the RNA volume of *idh3*), by which the expression level of *idh3* from 5 different samples is compared. The standards of five concentration levels which were diluted from the sample were used to produce two standard curves for target and housekeeping gene, respectively. After the reactions of the original samples and standards, the initial template amount of the target and housekeeping gene could be calculated when the Ct volume of the target or housekeeping gene was substituted in the standard curve of the target gene or housekeeping gene, respectively. Then all the samples were normalized by the corresponding housekeeping gene through a division of the quantitative results of the target gene by that of the housekeeping gene. Thus, *idh3* expression volume among the five samples was compared. To make the comparison of the gene expression volume between samples to be easier, the expression level of *idh3* in the control group was taken as "1", after which the relative amounts among the five samples were compared.

Bioinformatics analysis for IDH3

The tool, ProtParam (<http://us.expasy.org/tools/protparam.html/>), in ExPASy was used to analyze the negatively and positively charged residues of IDH3, the stability index of IDH3 and the hydrophobicity of IDH3. In addition, the simulative construction of the secondary and tertiary structures of IDH3 was implemented with the tool of Swiss-Port database (<http://expasy.org/sprot/>) by homology modeling algorithm.

RESULTS

Gene cloning for *idh3*

AFB₁ injected mice were anatomized and its liver was dissected, from which the total RNA was abstracted. The first strand cDNA was synthesized in accordance with the instruction in the reverse transcription kit from Promega, after which *idh3* was amplified with the first strand cDNA as the template. Finally, 5 L *idh3* amplification product was analyzed with the standard DL-2000 Marker by 1% agarose gel electrophoresis. The result of the electrophoresis is shown in Figure 1, in which there is a 1100 bp sized fragment that is consistent with the expected size. The result indicated that the amplification for gene *idh3* was successful.

The construction of prokaryotic expression vector pET28a-*idh3*

The restriction enzyme sites of *EcoRI* and *SaI* was added to the 5' and 3' ends of gene *idh3* respectively, with *idh3* cDNA as the template amplified by the corresponding primers. The pET28a and the gene *idh3* with two induced restriction enzyme sites were recovered after double digestion by *EcoRI* and *SaI*, after which they were connected by T4 ligase. Then, the recombinant plasmid was transformed into *E. coli* BL21. The kanamycin positive clones of *E. coli* BL21/pET28a-*idh3* was further identified by double digestion with restriction enzyme digestion, *EcoRI* and *SaI*, and was sequenced by Shanghai Yingjun Biotechnology Co., Ltd. The results

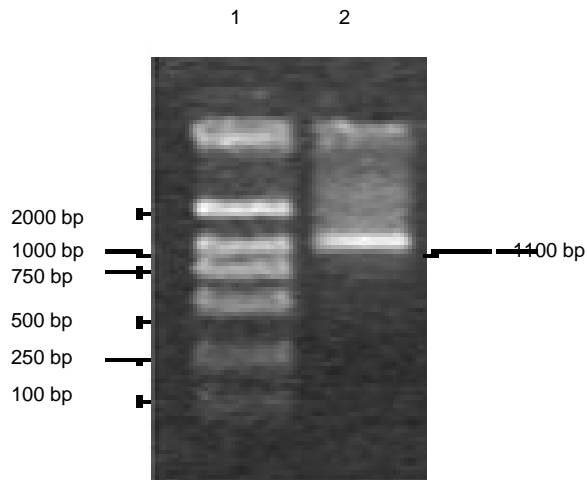


Figure 1. The amplification of *idh3* : 1. Marker; 2. *idh3* .

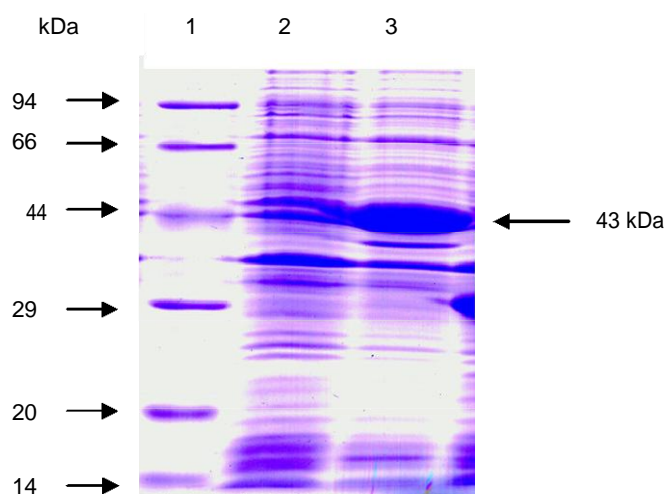


Figure 2. The SDS-PAGE analysis for the expression of IDH3 . Line 1: protein Marker; Line 2: *E. coli* BL21/pET28a(+) was induced by IPTG; Line 3: *E. coli* BL21/pET28a(+)-*idh3* was induced by IPTG.

indicated that the sequence of *idh3* was correct, and that *idh3* was inserted into the vector.

The prokaryotic expression for gene *idh3*

The *E. coli* BL21 strain with the identified expression vector (pET28a-*idh3*), and the strain with the empty vector (pET28a) were inducted to express at a final concentration of 100 mmol/L IPTG for 4 h, respectively. After induction, the pellet of *E. coli* BL21 cells was used to perform SDS-PAGE electrophoresis. The result indicated that a band of about 43 kDa which was identical with the theoretical value of IDH3 was found in the lane

of the strain with expression vector, while no corresponding band was found in the lane of the control strain (Figure 2), which indicated that IDH3 was successfully expressed.

Detection of the changing trend of *idh3* expression level by fluorescence quantitative PCR

The solution for fluorescence quantitative PCR was prepared, and *idh3* and *gapdh* were amplified according to the aforementioned process, after which the amplification curves of *idh3* were produced. The standard curves of *idh3* and *gapdh* were obtained, and it was seen that the standard curve for the reference gene, *gapdh*, was $y = 0.2846x - 4.10$, while that for the target gene, *idh3*, was $y = 0.2805x - 5.15$. Thus, the correlation coefficient for the standard curves of both genes were greater than 0.98 and their amplification efficiency was between 0.8 and 1.2. The relative quantification for *idh3* is shown in Table 2, and was calculated from the Ct value of the respective samples according to the algorithms introduced in "materials and methods". However, the dynamic changing trend of *idh3* is shown in Figure 3, according to the data given in Table 2. The results showed that the expression volume of *idh3* increased along with the elongation of the treating time of mice by AFB₁. These results corresponded to the result of our previous study through the method of differential proteomics analysis.

Bioinformatics analysis for IDH3

Analyzing IDH3 by the tool of ProtParam, it was predicted that the total number of negatively charged residues was 42 (Asp + Glu), and that of the positively charged residues was 39 (Arg + Lys). The instability index of IDH3 was computed as 39.90 which meant that the protein was stable. There were 5 hydrophobic domains predicted by the tool of ProtParam, and the average predictive value for IDH3 hydrophobicity was -0.069 (Figure 4). The results of the secondary and tertiary structure prediction by molecular simulation in Swiss -Port data base showed that there were 43% α -helix (159 residues) and 20% β -pleated sheet (73 residues) in IDH3, while the tertiary structure of IDH3 was constituted by 12 α -helices and 12 β -pleated sheets (Figures 5 and 6).

DISCUSSION

There are two ways to verify the difference expression protein discovered by proteomics: one is to directly test the changing trend of these proteins in the treating process, while the other is to validate the changing trend of these proteins indirectly (Ren et al., 2010). Immunohistochemistry is usually used in the former way, in

Table 2. The relative quantification of target genes.

Primer	Week				
	0	1	2	3	4
<i>idh3</i>	1.000	4.857	5.185	7.591	11.862

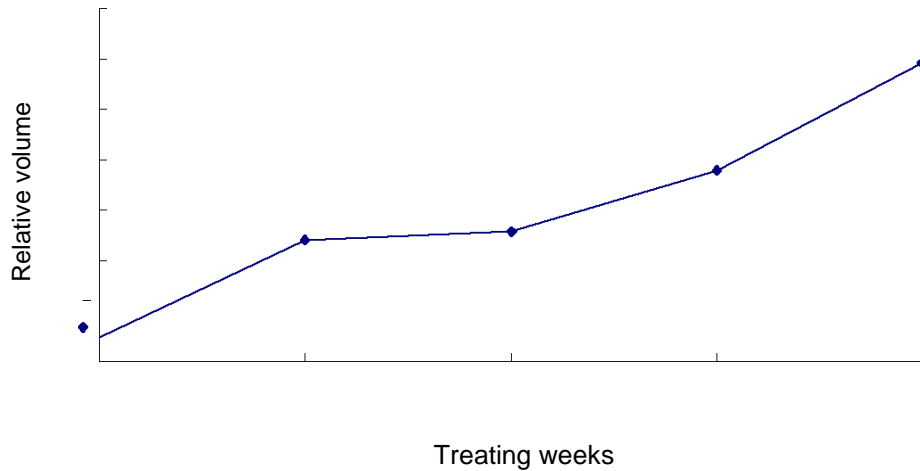


Figure 3. The dynamic map of the *idh3*.

which the labeled antibodies of corresponding protein were prepared and used to detect the change of the protein's volume directly by reacting with tissue slices (Li et al., 2008). The changing trend of mRNA expression volume could be used as an indicator for the changing trend of corresponding protein, so fluorescence quantitative PCR was always used in the latter way (Deepak et al., 2007; Sharpe et al., 2008). The latter method is more convenient and time saving, so it was chosen to verify the result of previous proteomics analysis in the study. To the up-regulated protein, if its mRNA expression volume increased after AFB₁ injection, the result of previous proteome analysis could be confirmed; but if the volume of mRNA did not change after AFB₁ injection, which could not prove the validity of the result of proteome analysis, the protein expression volume could be improved by increasing the half-life of its mRNA. In this study, fluorescence quantitative PCR was carried out with the liver sample taken from mice injected intraperitoneally with AFB₁ to detect the changing trend of *idh3* mRNA. The result showed that with extension of the AFB₁ exposure time, the amount of *idh3* mRNA tended to increase, which was consistent with the previous proteomic results. The result of the fluorescence quantitative PCR analysis confirmed that the expression volume of the protein, IDH3, could be induced by AFB₁. Thus, under the press of AFB₁, the expression volume of IDH3 would increase.

It was reported that IDH1 and IDH2 had a close relationship with tumor (Ward et al., 2010; Watanabe et

al., 2009), but there were no reports about the relationship between IDH3 and cancer. According to the "Warburg hypothesis", the cancer is quite different from normal cells in the aspect of metabolism, which means that high rates of aerobic glycolysis are maintained in cancer cells, and even the partial pressure of oxygen is as high as 20% (Warburg et al., 1956; Kondoh et al., 2005; Dang et al., 1999). Moreover, IDH3 is a mitochondria protein (Hartong et al., 2008). According to the hypothesis, the expression level of IDH3 should be decreased, but the result of the research was just opposite to it. Palmfeldt et al. (2009) found that when fibroblast cultures were cultivated in galactose medium, a metabolic stress and mitochondria number appeared to be maintained, whereas the expression volume of some proteins were altered. NAD-dependent isocitrate dehydrogenase (IDH3) of the TCA cycle was observed with a 26% increment, and it was one of the cellular strategies used to cope with the altered energy metabolism (Palmfeldt et al., 2009). It was reported that the transcription hypoxia-inducible factor 1 (HIF-1) was implicated in tumor angiogenesis and tumor-cell glycolysis. Proline hydroxylases that suppress the expression of (HIF-1) require -ketoglutarate as a substrate. Therefore, the inactivation of IDH could promote the accumulation of HIF-1 (Thompson et al., 2009). So it tips that the over-expression of IDH3 may be a mechanism for cells to suppress canceration under AFB₁ stress, but the exact role of IDH3 in the process of carcinogenesis

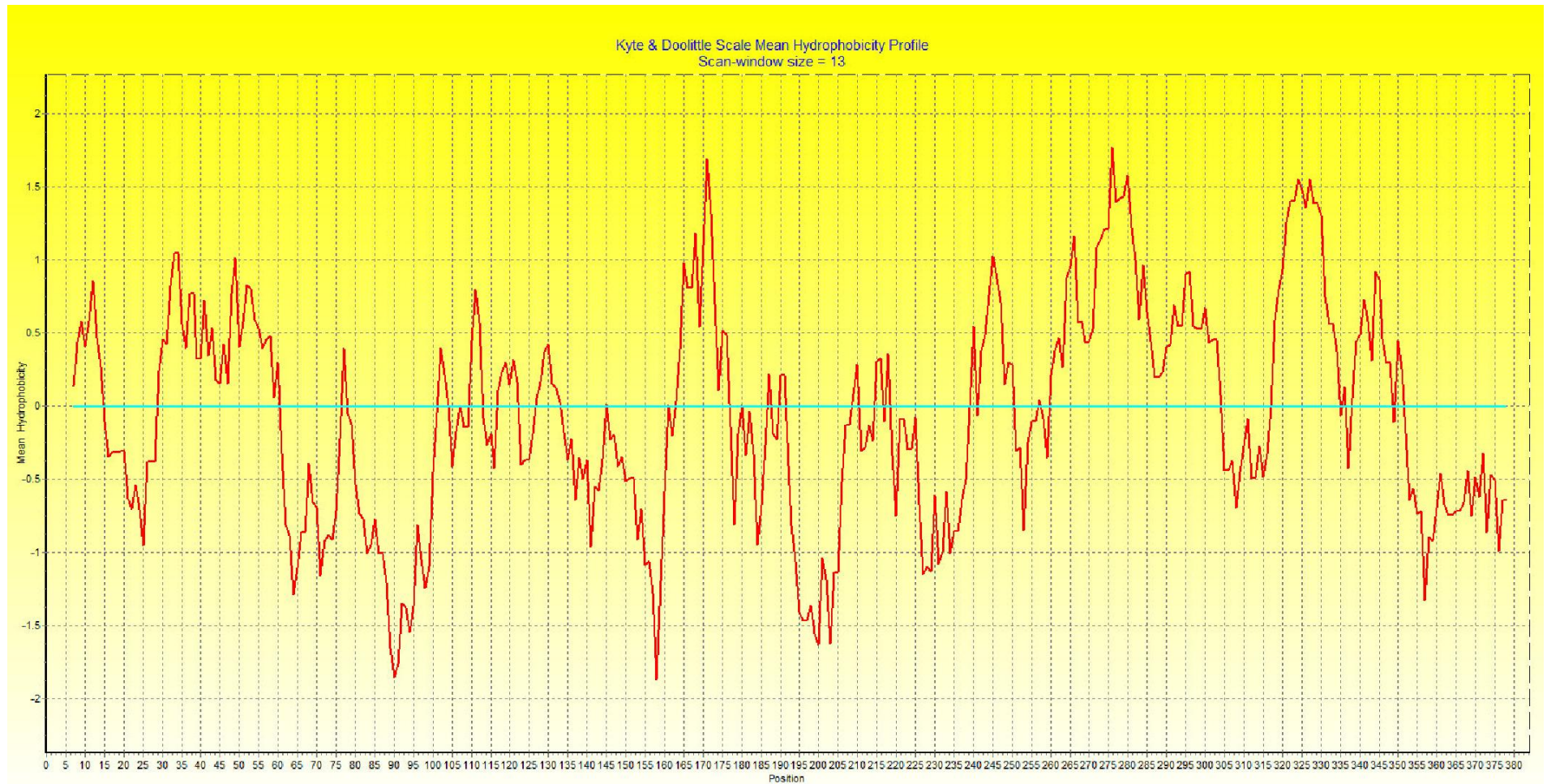


Figure 4. Hydrophobicity analysis of IDH3 .

under the stress of AFB₁ needs further study. Our lab plan was to use immunohistochemical and immunoprecipitation techniques to further clarify the function of IDH3 in mice under the press of AFB₁. For this purpose, a prokaryotic expression

system for *idh3* was constructed, and IDH3 was successfully expressed.

To further improve the titer of anti- IDH3 polyclonal antibody, bioinformatics analysis was carried out in the experiment to predict the residue

charge character, stability, hydrophobicity, and secondary and tertiary structure of IDH3 . An ideal epitope is generally subjected to the following features: (1) Hydrophilic fragment; (2) Accessible fragment (most of the antibodies are

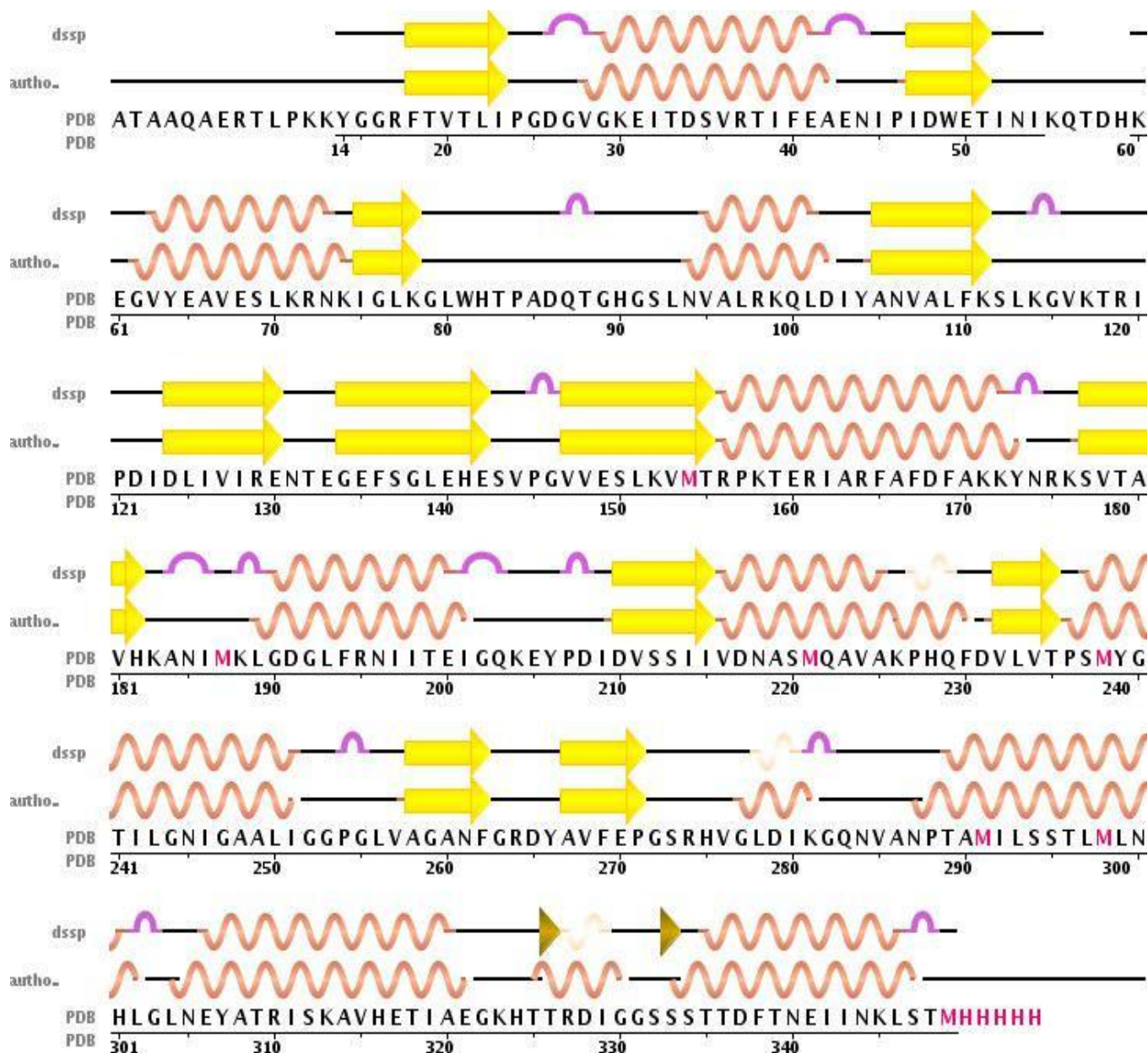


Figure 5. Prediction for secondary structure of IDH3 . 43% α -helix (12 helices; 159 residues); 20% β -pleated sheet (12 strands; 73 residues).

bound only the surface part of the protein); (3) It is generally believed that beta-turns are more likely to be epitopes because they always appear on the protein surface, but the structure of alpha-helix and beta-pleated sheet are more rigid, in that they are difficult to be bound by antibodies; so, in normal condition, they are not to be considered as epitopes; and (4) The N- and C-terminal of a protein are always good choices to be considered as epitopes (Bartlett et al., 2003). Based on these principles, the fragment of 1-17 and 112-123 residues of IDH3 were selected as candidates for further effective polyclonal antibody preparation. The results of Bioinformatics

analysis would be helpful in anti-IDH3 polyclonal antibody preparation, which would avail the further clarification of the role of IDH3 in AFB₁ carcinogenesis of mice liver. These works laid a solid foundation for further research, including the changing model of IDH3 and the field of searching interacting proteins of IDH3 .

ACKNOWLEDGEMENTS

The authors sincerely appreciate the support from the National "863" Program of China (No. 2007AA10Z430),

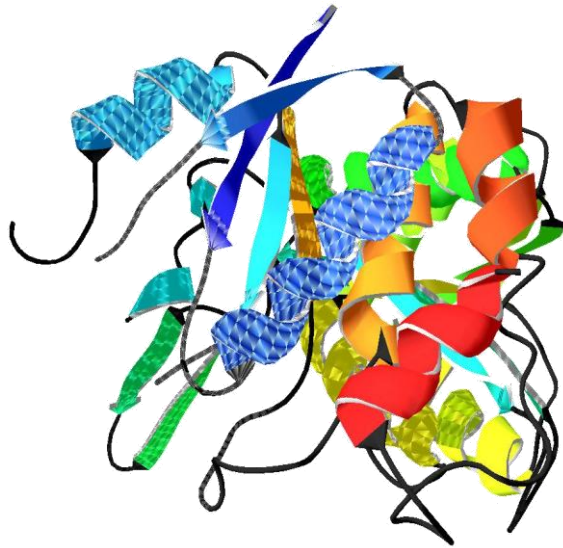


Figure 6. Prediction for tertiary structure of IDH3 .

the National Natural Science Fund Project (31000961, 30771400), the Nature Science Foundation of Fujian Province (2010J01068, 2009J06008), Program for New Century Excellent Talents in University (NCET-10-0010), the Eleventh Huo Yingdong Young Teacher Foundation Sponsorship for University (No. 111032), Key Project for Intellectual Introduction of Fujian Province (SZ2008039), Subsidizing Program for Provincial Universities of Department of Education of Fujian Province (JK2010022), Construction projects of Fujian Science and Technology Innovation Platform (2009Y2005), and by Program for New Century Excellent Talents in Fujian Province University.

REFERENCES

- Bartlett GJ, Todd AE, Thornton JM (2003). Inferring protein function from structure. *Methods Biochem. Anal.*, 44: 387-407.
- Chanda A, Roze L, Pastor A, Frame M, Linz JE (2009). Purification of a vesicle-vacuole fraction functionally linked to aflatoxin synthesis in *Aspergillus parasiticus*. *J. Microbiol. Methods*, 78(1): 28-33.
- Cho SA, Seo MJ, Ko JY, Shim JH, Yoo J, Kim JH, Kim SY, Ryu NK, Park EY, Lee HW, Lee YS, Bahk YY, Park JH (2010). Up-regulation of Idh3alpha causes reduction of neuronal differentiation in PC12 cells. *BMB Rep.*, 43(5): 369-374.
- Deepak SA, Kottapalli KR, Rakwal R, Oros G, Rangappa KS, Iwahashi H, Masuo Y, Agrawal GK (2007). Real-Time PCR: Revolutionizing Detection and Expression Analysis of Genes. *Curr. Genomics*, 8(4): 234-251.
- Dang CV, Semenza GL (1999). Oncogenic alterations of metabolism. *Trends Biochem. Sci.*, 24: 68-72.
- Hartong DT, Dange M, McGee TL, Berson EL, Dryja TP, Colman RF (2008). Insights from retinitis pigmentosa into the roles of isocitrate dehydrogenases in the Krebs cycle. *Nat. Genet.*, 40(10): 1148-1149.
- Hartong DT, Dange M, McGee TL, Berson EL, Dryja TP, Colman RF (2008). Novel insights into the contributions of isocitrate dehydrogenases to the Krebs cycle from patients with retinitis pigmentosa. *Nat. Genet.*, 40(10): 1230-1234.
- IARC (2002). Traditional herbal medicines, some mycotoxins, naphthalene, and styrene. *IARC Mon. Eval. Carcinogen Risk Hum.*, 82: 1-556.
- Kondoh H, Leonart ME, Gil J, Wang J, Degan P, Peters G, Martinez D, Carnero A, Beach D (2005). Glycolytic enzymes can modulate cellular life span. *Cancer Res.*, 65: 177-185.
- Li Z, Huang C, Bai S, Pan X, Zhou R, Wei Y, Zhao X (2008). Prognostic evaluation of epidermal fatty acid-binding protein and calcyphosine, two proteins implicated in endometrial cancer using a proteomic approach. *Int. J. Cancer*, 123: 2377-2383.
- Leema G, Kaliamurthy J, Geraldine P, and Thomas PA (2010). Keratitis due to *Aspergillus flavus*: Clinical profile, molecular identification of fungal strains and detection of aflatoxin production. *Mol. Vis.*, 16: 843-854.
- Ndiaye K, Fayad T, Silversides DW, Sirois J, Lussier JG (2005). Identification of downregulated messenger RNAs in bovine granulosa cells of dominant follicles following stimulation with human chorionic gonadotropin. *Biol. Reprod.*, 73(2): 324-333.
- Palmfeldt J, Vang S, Stenbroen V, Pedersen CB, Christensen JH, Bross P, Gregersen N (2009). Mitochondrial proteomics on human fibroblasts for identification of metabolic imbalance and cellular stress. *Proteome Sci.*, 7: 20.
- Ramachandran N, Colman RF (1980). Chemical characterization of distinct subunits of pig heart DPN-specific isocitrate dehydrogenase. *J. Biol. Chem.*, 255: 8859-8864.
- Ren F, Wu H, Lei Y, Zhang H, Liu R, Zhao Y, Chen X, Zeng D, Tong A, Chen L, Wei Y, Huang C (2010). Quantitative proteomics identification of phosphoglycerate mutase 1 as a novel therapeutic target in hepatocellular carcinoma. *Mol. Cancer*, 9: 81-97.
- Shephard GS (2003). Aflatoxin and food safety: recent African perspectives. *J. Toxicol.*, 22(2-3): 267-286.
- Sharpe RM, Dunn SN, Cahoon AB (2008). A plastome primer set for comprehensive quantitative real time RT-PCR analysis of *Zea mays*: a starter primer set for other Poaceae specie. *Plant Meth.*, 4: 14.
- Thompson B, Thompson CB (2009). Metabolic Enzymes as Oncogenes or Tumor Suppressors. *N. Engl. J. Med.*, 360(8): 813-815.
- Wogan GN (1966). Chemical nature and biological effects of the aflatoxins. *Bacteriol. Rev.*, 30(2): 460-470.
- Warburg O (1956). On the origin of cancer cells. *Sci.*, 123: 309-314.
- Wild CP, Gong YY (2010). Mycotoxins and human disease: a largely ignored global health issue. *Carcinogen*, 31(1): 71-82.
- Watanabe T, Nobusawa S, Kleihues P, Ohgaki H (2009). *IDH1* Mutations Are Early Events in the Development of Astrocytomas and Oligodendrogliomas. *Am. J. Pathol.*, 174(4): 1149-1153.
- Ward PS, Patel J, Wise DR, Abdel-Wahab O, Bennett BD, Collier HA, Cross JR, Fantin VR, Hedvat CV, Perl AE, Rabinowitz JD, Carroll M, Su SM, Sharp KA, Levine RL, Thompson CB (2010). The common feature of leukemia-associated IDH1 and IDH2 mutations is a neomorphic enzyme activity converting alpha-ketoglutarate to 2-hydroxyglutarate. *Cancer Cell*, 17(3): 225-234.
- Williams JH, Phillips TD, Jolly PE, Stiles JK, Jolly CM, Aggarwal D (2004). Human aflatoxicosis in developing countries: a review of toxicology, exposure, potential health consequences, and interventions. *Am. J. Clin. Nutr.*, 80(5): 1106-1122.
- Yin Y, Yan L, Jiang J, Ma Z (2008). Biological control of aflatoxin contamination of crops. *J. Zhejiang Univ. Sci. B.*, 9(10): 787-792.